BJES Basrah Journal for Engineering Sciences

Basrah Journal for Engineering Sciences, Vol. 26, No. 1, (2026), 26-34

Original Article

Journal homepage: https://bjes.edu.iq/bjes
ISSN (Online): 23118385, ISSN (Print): 18146120

IRAQI Academic Scientific Journals

Experimental Study of Boiling Heat Transfer in Zigzag and Symmetric Circular-Cavities Microchannels

Yamam Taqi Abed [1]*, Ahmed Jasim Shkarah [2]

[1] *Department of Mechanical Engineering, College of Engineering, University of Thi-Qar, Nasiriyah, Iraq*
E-mail addresses: yamam.t.a@utq.edu.iq , mymyalmhndst81@gmail.com , shkarah@utq.edu.iq

Article Info

Article history:
Received: 20 April 2026
Revised: 20 May 2026
Accepted: 16 Jun 2026
Published: 28 July 2026

Keywords:
Boiling, Microchannels, Symmetric circular-cavities, Zigzag microchannels.

https://doi.org/10.33971/bjes.26.1.4

Abstract

An experiment was conducted on two types of microchannels (zigzag and symmetrical circular) using water as the working fluid under normal boiling conditions. Heat fluxes ranging from 180 to 780 kW/m² were used, the Reynolds number varied from 58 to 107, and the water flow was streamlined. Temperatures were measured at ten ports (inlet, outlet, and walls). The results showed that for the zigzag channel at a heat flux of 580 kW/m², the average wall temperature decreased from 112°C to 87°C as the Reynolds number increased to 107. Both the Nusselt number (from 42 to 86) and the Reynolds number (from 58 to 107) also increased. The zigzag channel exhibited an improvement in heat transfer coefficient with a 30% decrease in the average temperature. The temperature of the circular cavity channel decreased from 126°C to 96°C, while the flow remained constant. Flow patterns were captured using a high-resolution camera for study during boiling.

1. Introduction

The flow of two phases in microchannels has become of great importance in many modern and advanced applications, such as electronics cooling, medical genetic engineering, bioengineering, chemical engineering, and micro-electro-mechanical systems. For these reasons, this topic has recently attracted the attention of researchers and has become the focus of their attention for experimental and numerical studies. Research papers have been published by the Research Committee in this field on fluid flows in micro channels and heat transfer, organized by the Japanese Society of Mechanical Engineers [1]. Information and studies related to heat transfer and flows at the microscale of less than 100 are in great demand. In order to evaluate practical performance and engineering design, it is necessary to know a number of basics related to the flow of two phases in very small (one micron) and small (less than a millimeter) passages. These basics include the vacuum and its ratio, flow and its patterns, pressure and its drop, the liquid film and its thickness, etc. Ghiaasiaan and Abdel-Khalik [2] and Serizawa and Feng [3] presented the heat transfer and two-phase flows inside micro channels in particular in a more extended and developed manner. Furthermore, knowledge on this subject is scarce despite the studies that have been presented in this field. There are many questions that need to be answered, such as whether the two-phase flow patterns in microchannels differ from those in conventional channels. In conventional tubes of standard size, gravity and surface tension are the dominant forces in two-phase flow patterns, with little effect. The same applies to microchannels. In small channels, ranging in size from microns to tens of microns, inertia, viscous forces, and surface tension are particularly affected. Maharudrayya et al. [4] conducted a numerical study using carbon dioxide gas inside the zigzag channel. The results showed that this channel increases heat transfer even when the pressure loss increases. Huang et al. [5] conducted an experimental study on circular channels with symmetrical cavities. The results showed that these channels have lower pressure losses and improved heat transfer compared with the straight channel. Tu and Zeng [6], Reduced the bending angle and zigzag length improves heat transfer in the zigzag channel and reduces pressure losses. Hou and Xu [7] conducted a numerical and experimental study of channels of various shapes, which were precise and contained cavities. The results showed that the circular channels generated vortices. These vortices helped in improving heat transfer and the pressure losses were small, which led to improving the cooling process and its efficiency. Lee et al. [8] conducted a numerical study on types of winding channels with different curvature angles 10 and 40. This study concluded that thermal performance is better at angles of 20, accompanied by an increase in pressure losses and heat transfer. Staszak and Musielak [9] conducted a numerical and analytical study concluded that the channel that achieves the best cooling for electronics is the rectangular winding channel, by improving heat transfer with an existing increase in pressure losses. Mathew et al. [10] conducted through experimentation, they proved that the best heat transfer occurs in the zigzag channel when compared to the straight channel, but there is an increase in pressure losses and they are small. Li et al. [11] performed a numerical and experimental study. The working fluid used was Al_2O_3-nanowater, and the heat exchanger was shaped precisely and contained internal cavities. The results showed that this design and the use of nanofluids contributed to a 38% improvement in heat transfer and a temperature reduction compared to a straight channel. However, most of the studies focused on different channels such as straight or zigzag, as well as the use of nanofluids as a working fluid. However, this study focused on zigzag, circular and symmetrical channels, and only water was used as a working fluid under the same conditions. Therefore, the main goal of this experiment is to know the heat transfer characteristics in zigzag and circular symmetrical channels and compare them if the working fluid used is water and the heat flux is between (180 – 780) kW/m^2. The primary objective of this study stems from the significant challenges faced by high-power microelectronic devices, which generate high temperatures that conventional cooling systems are unable to effectively cool. In microchannel flow boilers, the latent heat of vaporization can be utilized to cool these small devices. However, despite these advantages, microchannels also suffer from problems such as premature drying and flow instability. This research presents a comparison of two types of channels: zigzag channels, which promote mixing and generate secondary eddies, and symmetrical perforated channels, which contain cavities that enhance localized mixing. By comparing these two configurations at heat flows up to 780 kW/m², this study provides crucial insights into the performance of boiling heat transfer while ensuring that the critical heat flow is not reached.

2. Experimental work

In this research, an experiment was conducted on zigzag channels and symmetrical circular channels, and the dimensions of each channel were as follows: the width of the channel was w_c = 0.27 mm while the thickness of the half wall was calculated through 0.5 × w_c and was 0.135 mm while the length and height of the channel were L_c = 30 mm, H_c = 0.72 mm respectively and the hydraulic diameter of the channel was H_c = 0.39 mm while the dimensions of the disperser base were L_m = 30 mm while the width of the disperser base was w_m = 10 mm. The working fluid used was water. The channels were made of copper due to its specifications that qualify it for manufacturing (thermal, mechanical, and chemical properties, economic aspects, and application). The copper was formed using a wire-cutting machine, and the shaping process was carried out using a CNC machine, in addition to laser engraving and cutting. There are nine openings in the bottom of the channel for the insertion of cylindrical heaters. These heaters operate at 60 watts, and the voltage required for each heater is 24 volts, all to achieve the boiling process. The channel walls are relied upon to control thermal leakage. Insulation is done with thermal wool. The ceiling and base are not insulated, as the base contains the heaters, and the ceiling is fixed on a piece of heat-resistant glass. The overall structure consists of ten openings in these openings. To measure the water temperature, temperature sensors are placed at the inlet and outlet, while the remaining eight are located on the right and left sides, there are 4 on each side to measure the water temperature, as well as the walls of the channel.

2.1. Engineering description of channels

2.1.1. Zigzag channel

The zigzag heat sink has the same dimensions as the one mentioned above, and also contains seventeen zigzag channels, as shown in Fig. 1. The zigzag modules shown in Fig. 2 have a zigzag angle of 180 degrees.

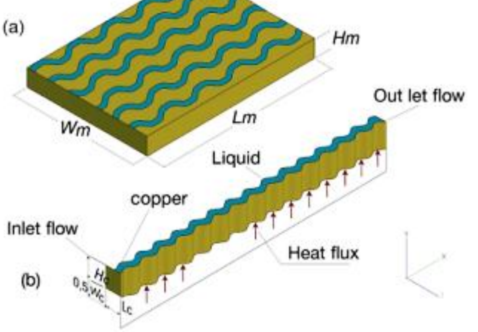

Fig. 1 (a) zigzag microchannel heat sink, **(b)** ZMHS unit.

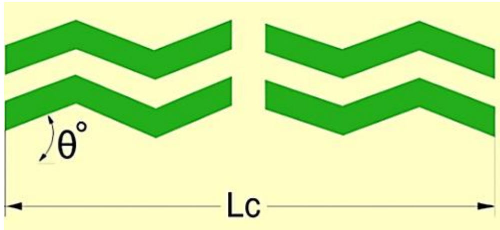

Fig. 2 The zigzag microchannel from the top view.

2.1.2. Circular cavities microchannels

This is the basic structure upon which this work is based. It consists of twelve channels with the same dimensions as previously mentioned, as shown in Fig. 3. The heat sink features symmetrical circular cavities, as shown in Fig. 4. This channel features circular cavities with symmetrical grooves distributed along the channel, and the radius of each groove R is 0.86 mm.

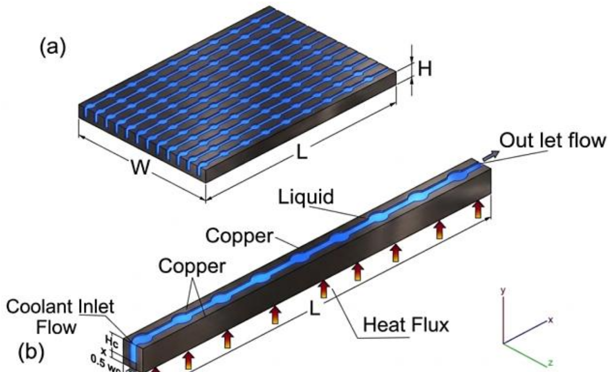

Fig. 3 (a) symmetric circular cavities microchannel heat exchangers. **(b)** MCHS-SCC unit.

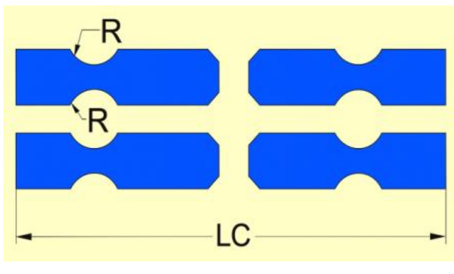

Fig. 4 Microchannel heat exchangers with symmetrical circular cavities from the top view.

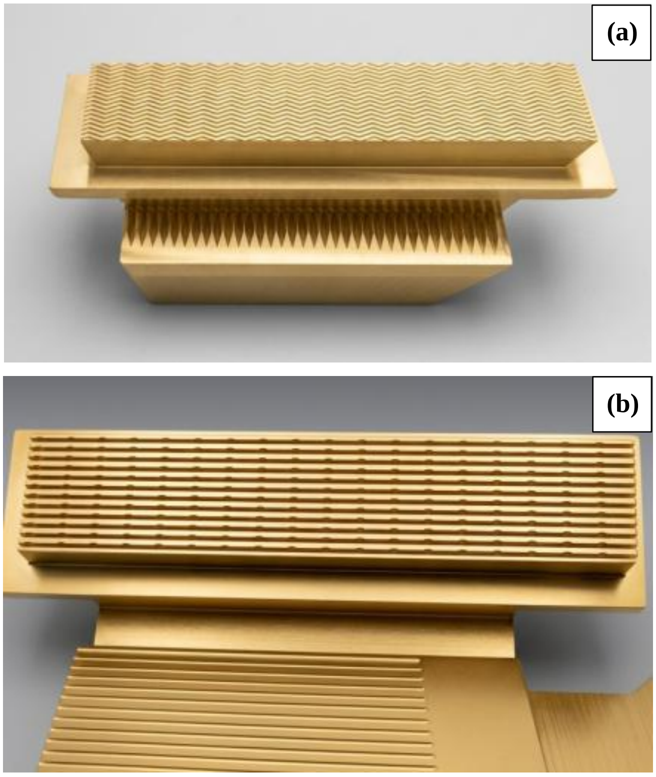

Fig. 5 The shape of the channel after the manufacturing process, **(a)** zigzag micro-channel, **(b)** symmetric circular cavities.

2.2. *Experimental setup*

2.2.1. Experimental work devices.

The following components are the tools that make up the device and are shown in Figs. 6 and 7. The main part of the experiment is the heat sink, or what is called the heat exchange unit. In this part, boiling occurs and heat is transferred. The water is stored in a tank and a valve is connected to it to control the flow rate inside the channel. The water is delivered to all parts of the experiment through connecting pipes. The water must be purified of contaminants before entering the channel. The water is purified in the purification unit. To accurately measure the temperature in each part of the channel, a K-type thermocouple is used. To monitor the temperature, these sensors are connected to a digital temperature monitor with units for collecting readings. The water is pushed into the channel using a drive pump.

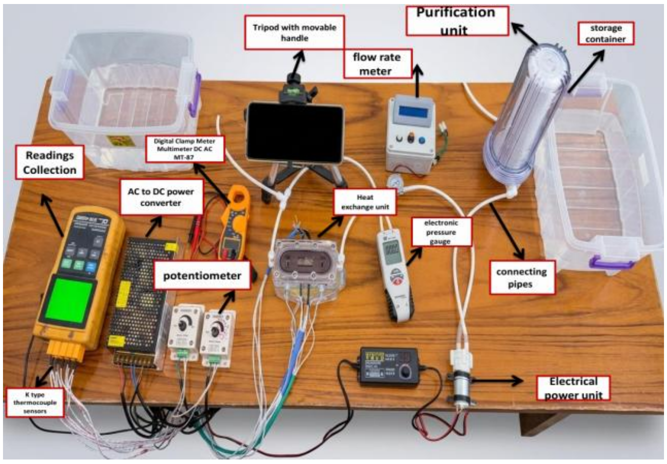

Fig. 6 Experimental work devices.

The electrical power unit consists of a device that converts alternating current to direct current and a new meter to adjust the applied voltage. The pressure at the inlet and outlet is measured by an electronic pressure gauge, and the amount of flowing water is measured by a flow rate meter. A flexible tripod is used to install the device (iPhone 16 Pro Max camera) used to film the boiling process. A digital multimeter is used to calculate the heat flux by measuring current and voltage.

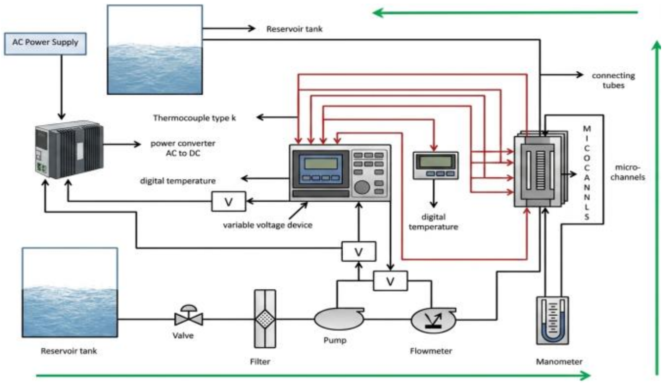

Fig. 7 A schematic diagram showing the experimental components that were used in the experiment.

2.3. Fluid movement within the channel

The experiment proceeds as follows: There is a tank containing the working fluid, which is water. A valve is installed and connected to the tank to control the amount of water. There is a filter used to purify the water from impurities, and the water flow is measured using a flow meter. The water is pumped using a pump to control the amount of water flowing according to the Reynolds number of 58 and 107. The water is pumped at a temperature of 300 K. The water then enters the test section. Here, heat exchange occurs, and as a result, the water temperature rises due to the heat absorbed from the walls. There are heaters inside the channels that help raise the temperature of the walls and bring them to a boil. The water is then released and collected in a second tank. The water temperature is measured by ten temperature sensors: one at the inlet, one at the outlet, and eight on the channel walls.

2.4. Steps to follow for conducting the experiment

A series of experiments were conducted to determine the effect of the geometric shapes of the microchannels (circular and zigzag) on the performance of the heat sink. The Reynolds numbers used were from 58 to 107. The fluid used in the experiment was water. The steps are as follows:

The first tank is filled with water, and the flow of water coming from the tank is controlled by a valve. The tank is equipped with a filter to purify the water entering the channel from impurities, and a device to measure the amount of water flowing. The water is pumped through a pump to enter the test section.

The channel is heated using cylindrical heaters placed at the base of the channel, and the temperature is controlled by a voltage regulator. The heat flux ranges between 170 and 780 kW/m^2.

The voltage regulator is regulated based on the experimental conditions. Water then enters the channel, heat exchange occurs, and the water coming out of the channel is collected in a second tank.

The temperature is measured using a number of K-type thermal sensors. Ten: one at the exit, one at the point of entry, and eight at the walls.

2.5. Experimental procedure and operational criteria

In this experiment, before data recording, the system was strictly controlled to ensure it reached a stable state. The pump and the electrical power supply were adjusted to remain within the specified Reynolds range 58-107 and to achieve the desired heat flux. The system was operated for 35-40 minutes, and the billet was recorded if the temperature change measured by the thermocouples was less than ±0.1°C and the duration was at least five minutes continuously. In this case, the system remained within the stable laminar flow zone. The onset of nuclear boiling was determined either by photographing the transparent glass cover and observing it until bubbles appeared on the channel walls, or by the temperature stabilizing and ceasing to rise, as this indicates that the heat is now being directed towards water evaporation rather than raising the metal temperature.

3. Data reduction and experimental calculations

In this experimental study, primary experimental data of temperature, voltage, current, and volumetric flow were collected and processed using standard fluid mechanics and thermodynamic equations to determine the heat transfer characteristics within the microchannels that were extracted.

Heat flux

During the boiling process, it is necessary to calculate the amount of heat on the surface of the hot channel that is transferred to the liquid per unit area; therefore, this equation is used [12].

$$q'' = \frac{V.I}{A} \tag{1}$$

Heat transfer coefficient

Heat exchange is better if the heat transfer coefficient is high [13], and calculated by:

$$h = \frac{q''}{T_w - T_f} \tag{2}$$

Hydraulic diameter

The channels are not circular in shape, the actual diameter must be replaced with another diameter, which is the hydraulic diameter [14].

$$D_h = 4\frac{A_c}{p} \tag{3}$$

Reynolds number

This equation is used to determine the type of flow (laminar, turbulent, transitional) within the channel [15].

$$Re = \frac{\rho U D_h}{\mu} \tag{4}$$

Nusselt number

In order to link heat transfer by convection with heat transfer by conduction [16].

$$Nu = \frac{hD_h}{k} \tag{5}$$

3.1. Assumptions

A set of fundamental assumptions was established to form the general framework for this analysis, simplifying the experimental data and facilitating the mathematical processing. These assumptions are as follows:

1. *Definition of working fluid flows and geometry:* The geometry of the heat sinks was precisely defined and included:

- Zigzag microchannels.
- Microchannels with symmetrical circular cavities.

Water was used as the working fluid, taking into account the high wall temperatures that cause the flow to transition to a two-phase state.

2. *Acting forces and neglected factors:* Radiant heat exchange is minimal compared to convection, and effect was excluded. As is known, shear and surface tension forces are dominant in microchannels, the effect of gravity was neglected.
3. *Physical properties and mathematical representation:* Several factors were used to describe the thermal and hydrodynamic behavior of the working fluid. The constancy of several thermophysical properties of water throughout the experiment was assumed to facilitate analytical calculations without compromising the fundamental results. These assumptions collectively highlight the fundamental factors influencing thermal performance, disregarding secondary and peripheral complexities.
4. *Uniformity of Heat Flow:* The heat generated by cartridge heaters within the copper block is uniformly distributed along the two zigzag channels and the symmetrical circular cavities.

3.2. Uncertainty analysis

An analysis was conducted to ensure the accuracy of the results obtained, based on the method proposed by Holman, which can be expressed by the following equation.

$$W_R = \sqrt{\left(\frac{\partial R}{\partial x_1} W_1\right)^2 + \left(\frac{\partial R}{\partial x_2} W_2\right)^2 + \cdots + \left(\frac{\partial R}{\partial x_n} W_n\right)^2} \tag{6}$$

Where, $W_1, W_2, \ldots, W_n$ represent the uncertainties of the independent measuring instruments.

Table 1 shows the uncertainty in the measuring instruments.

Table 1. the uncertainty in the measuring instruments.

Properties	Type	Value	Unit
Temperature (T)	K-type thermocouples	± 0.5	°C
Volumetric flow rate ($\dot{V}$)	Volumetric flow meter	± 2.0	%
Voltage (V) and Current (I)	Digital DC power supply	±1.5	%
Heat flux (q″)	Propagated (Holman's Method)	±2.8	%
Heat transfer coefficient (h)	Propagated (Holman's Method)	±3.5	%
Nusselt number (Nu)	Propagated (Holman's Method)	±3.5	%

4. Results and discussions

This section presents the results for zigzag and circular channels. These results were obtained through practical experiments. Different heat fluxes, ranging from 180 to 780 kW/m², were used. Temperatures were measured at the channel inlet and outlet, as well as on the channel walls. The results are presented graphically, illustrating the difference between these two channels and which performed better in terms of cooling and thermal conductivity. The channels were photographed at each heat flux. One of the most important results obtained is an inverse relationship between wall temperature and pump speed (the higher the pump speed, the lower the wall temperature). This means that flow rate affects thermal convection, with thermal convection improving as the flow rate increases. This means that wall temperature decreases as the water speed to facilitate reading and displaying the results, three readings will be taken: minimum heat flow 180, average heat flow 500 kW/m^2, and high heat flow 780 kW/m^2.

4.1. Effect of exit temperature

Figures 8, 9, and 10 illustrate how the outlet temperature changes with the Reynolds number in both zigzag and symmetrical circular channels at three flow levels: 180 kW/m² in Fig. 8, 500 kW/m² in Fig. 9, and 780 kW/m² in Fig. 10. In all these heat fluxes, the outlet temperature decreases as the Reynolds number increases. This is because the fluid's residence time within the channel decreases with increasing Reynolds number. When the Reynolds number is low (e.g., Re = 70), the fluid's residence time within the channel is long because the water velocity is low, allowing it to absorb more heat from the heated surface. However, if the Reynolds number is increased to 100 (e.g., Re = 100), the fluid's residence time within the channel decreases, resulting in a lower temperature. The outlet temperature in a zigzag channel is higher than in a symmetrical circular channel. This is due to the distinctive geometric shape of the zigzag canal. The sharp bends and continuous water movement cause the thermal boundary layer to break down and limit its development, thus raising the exit temperature because the amount of absorbed heat is higher. In contrast, in a canal with symmetrical circular cavities, the exit temperature is lower because it contains stagnant zones and localized cavities. Therefore, the zigzag canal is superior to the canal with symmetrical circular cavities in design.

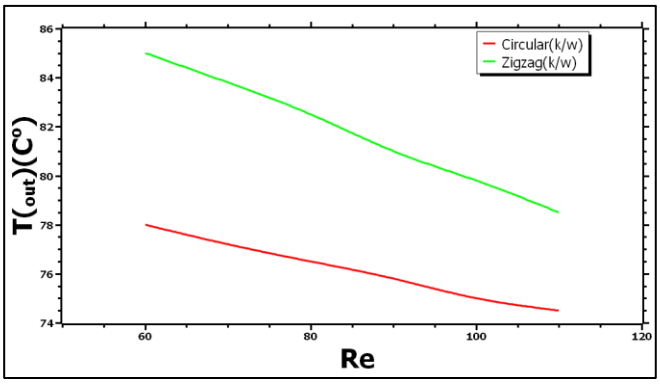

Fig. 8 Effect of a change in the Reynolds number on the outlet temperature of the zigzag and symmetrical circular-cavity channels at a heat flux of 180 kW/m².

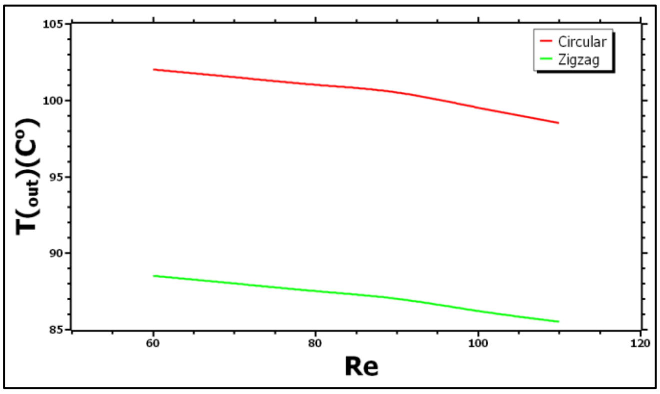

Fig. 9 Effect of a change in the Reynolds number on the outlet temperature of the zigzag and symmetrical circular-cavity channels at a heat flux of 500 kW/m².

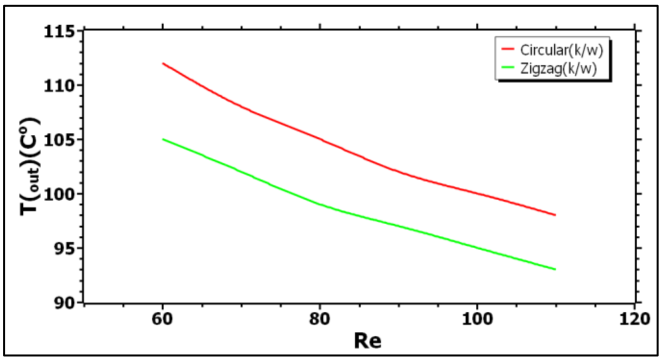

Fig. 10 Effect of a change in the Reynolds number on the outlet temperature of the zigzag and symmetrical circular-cavity channels at a heat flux of 780 kW/m².

4.2. Effect of average wall temperature

In all three Figures 11, 12, and 13, the change in average wall temperature with respect to the Reynolds number is observed at the three heat flow rates (180, 500, and 780 kW/m²). The average wall temperature decreases as the Reynolds number increases due to a higher convection coefficient at higher fluid velocities, resulting in increased heat dissipation. The average wall temperature in a channel with symmetrical circular cavities is higher than the average wall temperature in a zigzag channel under the same conditions. The reason for this is that in a tortuous channel there is random mixing of the fluid, continuous twists and secondary eddies that are generated, which leads to the breaking of the thermal boundary layer, which means that the fluid layers are constantly renewed at the walls of the channel and cause a decrease in the average temperature of the walls. Conversely, a channel with symmetrical circular cavities contains stagnant areas that are localized, and these areas cause the thermal boundary layer to accumulate on the walls of the channel, causing an increase in the average temperature of the walls and a decrease in cooling efficiency.

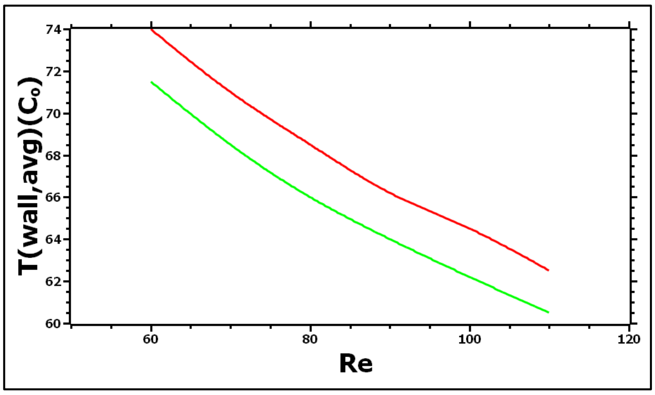

Fig. 11 Effect of a change in the Reynolds number on the average wall temperature of the zigzag and symmetrical circular-cavity channels at a heat flux of 180 kW/m².

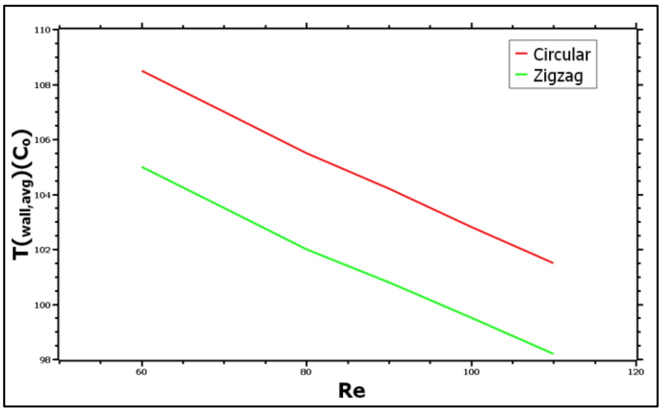

Fig. 12 Effect of a change in the Reynolds number on the average wall temperature of the zigzag and symmetrical circular-cavity channels at a heat flux of 500 kW/m².

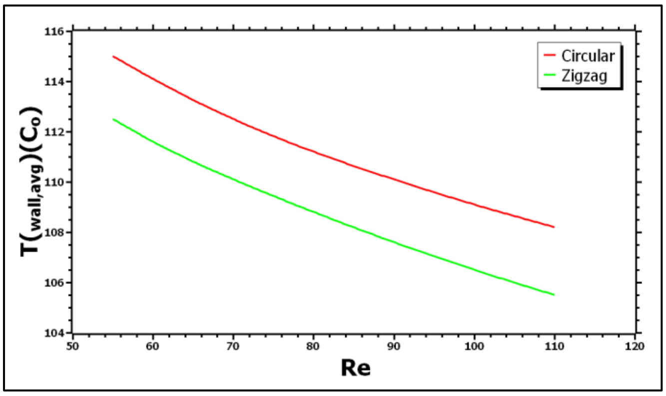

Fig. 13 Effect of a change in the Reynolds number on the average wall temperature of the zigzag and symmetrical circular-cavity channels at a heat flux of 180 kW/m².

4.3. Heat resistance effect

Figures 14, 15, and 16 illustrate the change in thermal resistance with respect to the Reynolds number. As the Reynolds number increases across the three heat flow rates 180, 500, and 780 kW/m², the thermal resistance decreases. This is because the heat transfer coefficient increases with increasing flow rates, which is accompanied by a decrease in resistance to convection. The thermal resistance values in a zigzag channel are lower than in a channel with symmetrical circular cavities. This is also due to the distinctive geometry of the zigzag channel, the continuous mixing of fluid layers, and the breakdown of the thermal boundary layer at the channel walls. In contrast, a channel with symmetrical circular cavities experiences stagnation due to localized cavities, resulting in a higher thermal resistance than a zigzag channel. Consequently, the thermal efficiency of a channel with symmetrical circular cavities is lower.

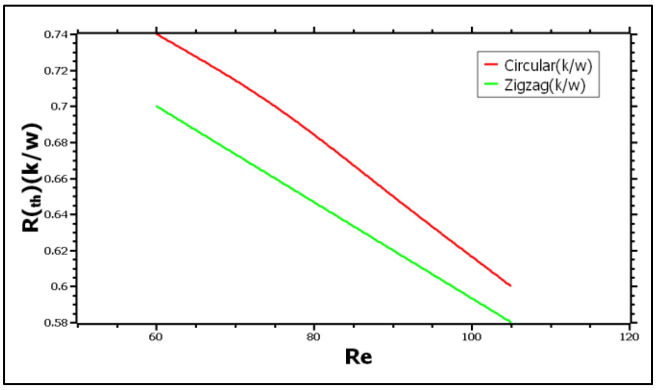

Fig. 14 Effect of changing the Reynolds number on the thermal resistance of the circular, symmetrical, and zigzag-shaped cavity channels at a heat flux of 180 kW/m².

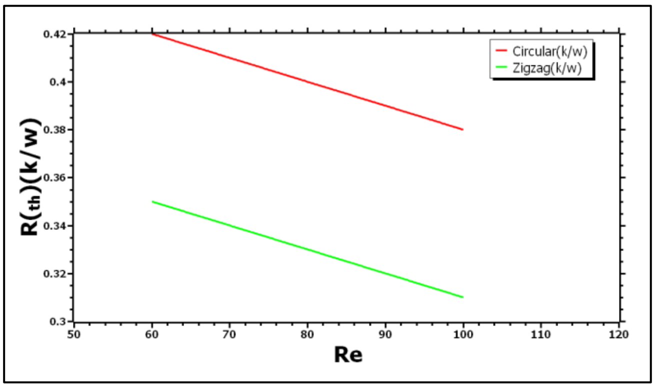

Fig. 15 Effect of changing the Reynolds number on the thermal resistance of the circular, symmetrical, and zigzag-shaped cavity channels at a heat flux of 500 kW/m².

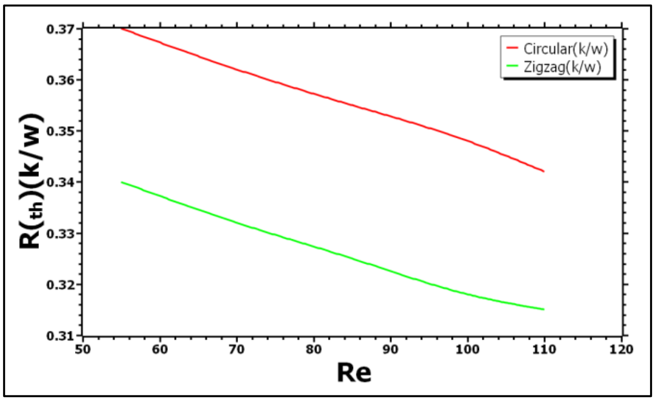

Fig. 16 Effect of changing the Reynolds number on the thermal resistance of the circular, symmetrical, and zigzag-shaped cavity channels at a heat flux of 780 kW/m².

5. Flow patterns

The flow patterns resulting from the boiling process within the zigzag and symmetrical circular channels are illustrated as water velocity and heat flow change. The main flow patterns were imaged using a high-resolution camera. Understanding these patterns is crucial for understanding fluid behavior within the channels, which in turn contributes to our understanding of heat transfer and its efficiency within microchannels.

5.1. Zigzag channel flow patterns

The mixing of the two phases is enhanced and the flow turbulence increases due to the sharp turns present in the zigzag channel, and this in turn is reflected in the flow patterns. When the heat flux is low $q'' = 180$ kW/m², the boiling pattern is in the form of bubbles. These bubbles appear on the channel walls, characterized by their small size and dispersed nature. They then merge, but this merging occurs earlier than in other channels due to localized turbulence. This merging happens at a heat flux of 220 kW/m². Subsequently, elongated bubbles form, and the flow becomes more turbulent at a heat flux of 260-300 kW/m². The most significant finding is that the transition to annular mode occurs earlier compared to straight and wave-like channels. The membrane becomes irregular due to repeated bends, and the annular mode is clearly visible at a heat flux of 340-400 kW/m². The membrane then becomes unstable until it ruptures at a heat flux of 500-560 kW/m² because, in annular flow, there are liquid droplets within the vapor nucleus. Partial desiccation begins to appear at $q'' = 600$ kW/m², then progresses to complete desiccation when the heat flux increases to 700-780 kW/m² due to significant losses in the liquid film. This occurs as a result of the sharp increase in evaporation rates and the resulting severe turbulence.

Fig. 17 Small scattered bubbles at a temperature of 180 kW/m².

Fig. 18 Clear irregular annular flow at heat fluxes 500 kW/m².

Fig. 19 There is a significant loss of liquid film with almost complete drying at heat fluxes of 780 kW/m².

5.2. Symmetrical circular cavities channel flow patterns

The local vortices present (generated due to the presence of circular cavities) affect the flow behavior because they promote phase mixing. At low heat fluxes $q'' = 180$ kW/m², nuclear boiling occurs, and small bubbles begin to appear on the channel walls. As the heat flux increases to 220-260 kW/m², these small bubbles merge to form continuous, elongated bubbles. Hydrodynamic instability begins to appear at a flow level of 300 kW/m², and the flow becomes slightly turbulent. The annular pattern becomes pronounced and begins to form when the heat flux increases to 300 kW/m². At a heat flux of 400 kW/m², the thickness of the liquid layer begins to fluctuate. The annular pattern becomes very stable and pronounced at a heat flux of 500 kW/m². Partial drying then begins to appear when the heat flux exceeds 560-600 kW/m², and liquid droplets are lost within the vapor core. A sharp decline in heat transfer efficiency occurs when the walls dry intermittently, followed by complete drying of the liquid film at a heat flux of 700 kW/m². From the above, an important fact can be concluded: the initiation of boiling is more directly related to the heat flux applied to the channel walls than to the channel's geometric shape. This fact was derived from comparing the four types. For microchannels. At low heat flow $q'' = 180$ kW/m², nuclear boiling occurs in all geometries, although the geometry does influence later stages of flow development. In straight channels, the transition to drying is rapid with high heat flow, while in wave channels, drying is delayed due to the ability to retain wall moisture. This is caused by intense mixing and localized vortices. Consequently, the transition to advanced flow patterns occurs earlier in wave channels than in symmetrical circular channels and zigzag channels.

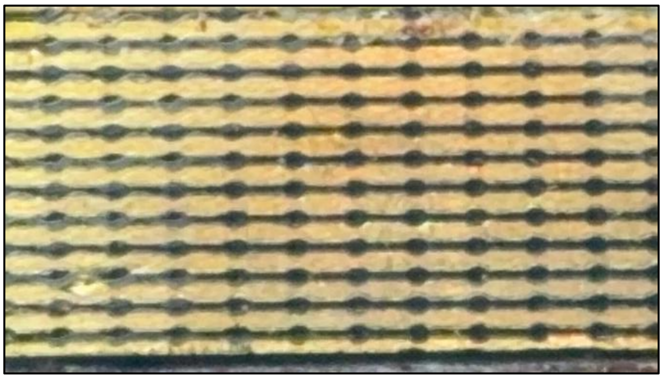

Fig. 20 Small scattered bubbles at a temperature of 180 kW/m².

Therefore, it can be said that wave channels are the best channels for combining enhanced heat transfer and delayed drying, followed by zigzag channels, and then symmetrical circular channels. The straight channel serves as a reference for other channels.

Fig. 21 Clarity in the annular flow at a heat flux of 500 kW/m².

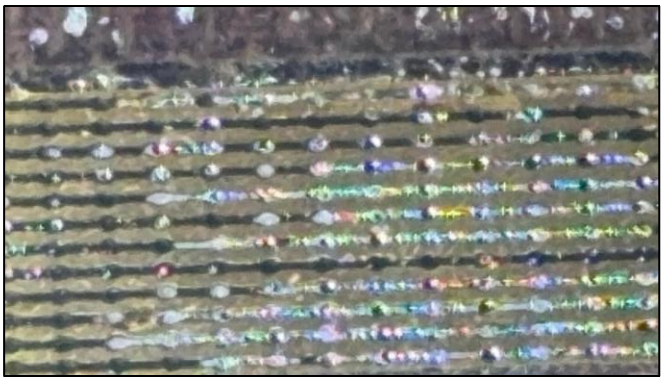

Fig. 22 The liquid film is dry at a heat flux of 780 kW/m².

6. Conclusion

The zigzag channel has numerous bends that aid in repeated mixing, resulting in improved heat transfer. This channel was the preferred choice at high heat flux 780 kW/m² and high thermal loads requiring high cooling. The symmetrical circular channel, however, was less effective than the zigzag channel, as it offered moderate and stable thermal performance and is a good choice for applications requiring stable thermal performance. Cooling was better at higher fluid flow rates, as the higher the pump speed, the lower the wall temperature across all heat fluxes. Therefore, the channel arrangement, from best to least cooled, is a zigzag and circular cavity due to the increased mixing within the channel and increased thermal layer breakage. Based on the above results, several conclusions can be drawn, the most important of which is that the zigzag channel is better than the symmetrical circular channel when used for future design purposes, especially under high thermal loads. It achieves a significant improvement in heat transfer, and its advantages make it the preferred channel for advanced precision cooling applications The primary reason for the superiority of the zigzag channel over the channel with symmetrical circular cavities, and the observed improvement, is due to several factors. The most important is that the zigzag channel, due to its unique geometric shape, experiences secondary flow generation, leading to significant fluid mixing due to the sharp bends in the zigzag channel. This mixing, in turn, leads to the continuous renewal and breakdown of the thermal boundary layer near the channel walls, resulting in a decrease in the average wall temperature for the zigzag channel. This indicates that random movement of the boiling fluid is crucial, as it helps remove and separate bubbles from the fine channel walls. This, in turn, prevents the formation of an insulating vapor layer, thus improving the local boiling heat transfer coefficient. To further develop this experimental work and make it comprehensive, encompassing the friction coefficient, energy loss, and pressure drop, a hydraulic analysis will be conducted to achieve a balance between fluid direction resistance and improved heat transfer in the zigzag channel.

7. Recommend future works

1. Use other geometric shapes, such as triangular, hybrid, and other shapes, to determine their impact on the boiling process and heat transfer.
2. It is important to use 3D simulation programs such as ANSYS and COMSEL to achieve high heat transfer efficiency and minimal pressure loss.
3. The channel surface can be modified, as it is of great importance in improving heat transfer.
4. The current study used water as the working fluid, so nanofluids could be used in the future.
5. There are temperature changes and vibrations during boiling, so it is possible to conduct studies on unsteady boiling states.
6. It is essential to conduct a comprehensive hydraulic analysis that considers both the friction coefficient and pressure drop in the zigzag channel.

References

[1] A. Serizawa, "Fluid flow and heat transfer in microchannels", JSME Report, Research Committee on Heat Transfer and Fluid Flow in Microchannels, P-SC295, 2001.

[2] S. M. Ghiaasiaan and S. I. Abdel-Khalik, "Two-phase flow in microchannels", Advances in Heat Transfer, Vol. 34, pp. 145-254, 2001. https://doi.org/10.1016/S0065-2717(01)80012-5

[3] A. Serizawa and Z. Feng, "Review of two-phase flow in microchannels", in Proc. of the US–Japan Seminar on Two-Phase Flow Dynamics, Santa Barbara, CA, 2000.

[4] G. Maharudrayya, S. Jayanti, and A. P. Deshpande, "Pressure drop and heat transfer in zigzag channels", Experimental Thermal and Fluid Science, Vol. 32, Issue 1, pp. 283-291, 2007. https://doi.org/10.1016/j.expthermflusci.2007.03.004

[5] B. Huang, H. Li, and T. Xu, "Experimental investigation of the flow and heat transfer characteristics in microchannel heat exchangers with reentrant cavities", Micromachines, Vol. 11, Issue 4, p. 403, 2020. https://doi.org/10.3390/mi11040403

[6] Y. Tu and Y. Zeng, "Numerical study on flow and heat transfer characteristics of supercritical CO_2 in zigzag microchannels", Energies, Vol. 15, Issue 6, p. 2099, 2022. https://doi.org/10.3390/en15062099

[7] T. Hou and D. Xu, "Flow and Heat Performance of Microchannel Heat Sinks with Concave Cavities to Water-Cool Leds", SSRN Electronic Journal, 2023. https://doi.org/10.2139/ssrn.4617565

[8] Y. Lee, S. Lee, H. B. Park, K. W. Seo, and D. Lee, "Thermal-hydraulic performance analysis of zigzag channel PCHE according to bending angle", in Proc. of the Korean Nuclear Society Spring Meeting, Jeju, Korea, May 9-10, 2024.

[9] M. Staszak and G. Musielak, "Numerical simulations of flow and heat exchange in zigzag-shaped microchannels", Applied Sciences, Vol. 14, Issue 21, p. 9826, 2024. https://doi.org/10.3390/app14219826

[10] B. Mathew, F. Alnaimat, A. G. Hussain, S. Atatreh, B. M. S. Kakah, and Y. A. Ali, "Nusselt number and friction factor in zig-zag microchannels subjected to constant heat flux", International Journal of Thermofluids, Vol. 26, p. 101079, 2025. https://doi.org/10.1016/j.ijft.2025.101079

[11] F. Li, Z. Tan, H. He, Y. Zhou, X. Tang, and W. Zhu, "Research on thermal performance of the microchannel with internal cavities under Al_2O_3-water nanofluid", Energies, Vol. 18, Issue 16, p. 4419, 2025. https://doi.org/10.3390/en18164419

[12] F. P. Incropera, D. P. DeWitt, T. L. Bergman, and A. S. Lavine, Fundamentals of Heat and Mass Transfer, 8th ed., New York: Wiley, 2017.

[13] J. P. Holman, Heat Transfer, 10th ed., New York: McGraw-Hill, 2010.

[14] W. M. Kays and M. E. Crawford, Convective Heat and Mass Transfer, 3rd ed., New York: McGraw-Hill, 1993.

[15] B. R. Munson, D. F. Young, T. H. Okiishi, and W. W. Huebsch, Fundamentals of Fluid Mechanics, 7th ed., New York: Wiley, 2013.

[16] A. Bejan, Convection Heat Transfer, 4th ed., New York: Wiley, 2013.